

Snake Method Enhanced using Canny Approach Implementation for Cancer Cells Detection in Real Time

Ahmad Chaddad, Camel Tanougast and Abbas Dandache

Laboratory of Design, Optimization and Modeling (LCOMS), University of Lorraine, Metz, France

Keywords: Cancer, FPGA, Implementation, Segmentation, Snake.

Abstract: Optical microscopy is widely used for cancer cell detection via biopsy. Unfortunately this technique requires a large number of samples to determine the grade of the cancer cells. Because time is critical in this operation, a search for a method to reduce the length of this process is important. One such method showing promise is the implementation of the snake method for cancer cell detection. Ideally, this method will aim toward minimizing cost while maximizing efficiency. Using optical microscopy at LCOMS, we performed a proof-of-concept study to distinguish between normal and abnormal cells. We developed a snake/active contour method by which several curves move within images in order to find normal/abnormal cell boundaries. Abnormal cell identification typically takes more than one hour; however. The implementation of field programmable gate array (FPGA) technology solves this problem. A novel embedded architecture of the snake method is developed for an efficient and fast computation of active contour used in high throughput image analysis applications, where time performance is critical. This architecture allows for a scalable and a totally embedded processing on FPGA of a large number of images. The architecture of the snake method is able to detect objects from images which have irregular shapes, such as carcinoma cell types. To demonstrate the effectiveness of the approach, the architecture is implemented on Xilinx ISE 12.3-FPGA technology using Verilog hardware description language (VHDL). The very promising results using Snake method implementation and real cancer cell images from optical microscopy demonstrate the potentials of our approach.

1 INTRODUCTION

Biomedical instrumentation is basic to accurate medical diagnose. Electronic devices and instrumentation for medical applications are now essential for the prevention, diagnosis, treatment and rehabilitation of patients' diseases. In recent years, the trend has been toward the miniaturization of such system; namely, we have seen the development of microelectronic integrated circuits in devices such as biomedical implants, pacemakers, defibrillators, etc. In addition, the robust nature of computer analysis and vision facilitate the monitoring of patient diagnoses e.g. medical imaging, such as: Scanner, X-Ray, fNIRS, fMRI and Microscope (Castanon 2007, Wang 2008). In our work, we focus on optical microscopy imaging to automatically detect cancer cells in real time using FPGA technologies. Several literature sources propose the dynamic segmentation method for detection of objects inside images (Cataldo 2010, Szilágyi 2011).

Meanwhile, one of these methods, the Snake method, possesses a very high degree of accuracy, especially in cancer cell detection. The Snake method algorithm consists of several iterations in order to achieve the goal of cell detection. The method utilizes several bio-images from the microscopy system and requires at least three minutes in each abnormal cell for detection. The main disadvantage of the algorithmic approach developed, is the high computing power required for application in reasonable time. It is within this context that a hardware implementation based on FPGA technology of the proposed method is considered in order to solve constraint of time. Unfortunately, Snake method is not easy to implement, so we integrated the Canny approach for external energy. While the snake method is based on both internal and external energies, the integration of the Canny approach allows us to more easily implement external energy. Limited work has been done for Snake implementation using FPGA

technology. In this work, we propose a new architecture/design with the snake method used as the core of the implement segmentation whose advantage lies in the parallelism for which computation time is critical. An effort was made to integrate Canny approach in external energy for active contour equation. The objective of this implementation is to achieve an Appropriateness Algorithm Architecture target to meet the performance needs in terms of computation time, high accuracy of cancer cell detection, and optimization of material resources for the embedded implementation on FPGA technology. Texture analysis applied on multispectral bio-image was done in LCOMS laboratory in order to make a classification between types of cancer cell (Chaddad 2011a). This analysis utilized different structural patterns as well as apparent textures to diagnose different grades of cancer malignancy. Our project operates on the interface between optical microscopy and a control center "computer". The control center receives data from the optical microscopy via a charged coupled device (CCD) camera. The sensitivity of this camera is about 1000 times that of conventional CCD cameras. It was developed for observation under a wide variety of circumstances, from very bright stop action situations to extremely low light fluorescence conditions. The exposure time can be selected within the range of 1/10000th of a second up to 5 minutes, and a unique real time background subtraction function makes it possible to eliminate fixed pattern noise from optics and shading when doing fluorescence. It has a built-in image memory and an RS-170 output for standard video connection and a SCSI interface for digital output and camera control. Liquid Crystal Tunable Filter (LCTF) is a special filter which allows capturing of 16 spectral bands between 500 nm and 650 nm with a 9.375 nm step size between each successive band (Chaddad 2012). Fig.1 presents the global block diagram of our proposed work.

This paper provides an architectural implementation of external energy using canny approach for fast active contour method in order to detect cancer cells as described in section 2. We report and discuss the results in section 3, and the conclusion is the subject of section 4.

2 METHODS AND MATERIALS

2.1 Active Contour Model "Snake"

Snake method has been widely applied in various object contour detection and object tracking. Two

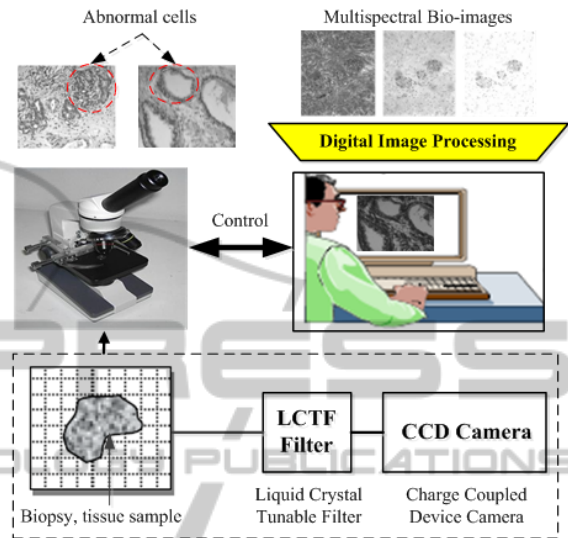


Figure 1: Block diagram of automatic cells detection via optical microscopy acquisition.

general types of active contour models have been proposed: the first is based on the minimization of the energy-functional associated to the model, as proposed by Kass (Kass 1988). The second is based on geometric models as proposed by Caselles (Caselles 1993) and the third is based on shape modeling as proposed by Malladi (Malladi 1995). Recently, utilization of deformable models and their applications can be found in medical imaging to detect cells or irregular shapes inside images (He 2008, Chen 2011). The energy function used by the snake to find contours can be expressed by the following equation:

$$E_{Snake} = E_{Internal} + E_{External} \quad (1)$$

where $E_{Internal}$ (internal energy) of the snake depends directly on the contour dot, which concerns several coefficients, such as curvature of the contour or correctness of dot spacing. In addition, the contour must retain a rounded shape by minimizing the derivatives of several orders (Chen 2012). Ideally, when the internal energy is minimum, all the points are reasonably spaced. This can be expressed by the internal spline energy in the following equation:

$$E_{Internal} = \frac{1}{2} [\alpha |V_s|^2 + \beta |V_{ss}|^2] \quad (2)$$

where V is the parametric curve of the active contour, $\|V_s\|^2$ is the first order measure of the elasticity, $\|V_{ss}\|^2$ is the second order measure of the curvature, α and β are the control coefficients.

The $E_{External}$ (external energy) of the snake represents the image & constraint forces. It can be expressed as Kass proposed it by the following equation:

$$E_{External} = w_{line}E_{line} + w_{contour}E_{contour} + w_{term}E_{term} \quad (3)$$

where W_{line} , $W_{contour}$ and W_{term} are regulator factors. In our work we set $W_{line} = W_{contour} = W_{term} = 1$.

- $E_{line} = I(x,y)$, is the line energy representing the pixel intensity.
- $E_{contour} = -|\nabla I(x,y)|^2$, is the contour energy representing the negative of square intensity gradient.
- $E_{term} = \frac{c_{xx}c_y^2 - 2c_{xy}c_xc_y + c_{yy}c_x^2}{(c_x^2 + c_y^2)^{\frac{3}{2}}}$, is the term energy

which depends on 5 coefficients c_x , c_y , c_{xx} , c_{yy} and c_{xy} . These coefficients are parallel and independently computed. Each coefficient is the result of a convolution between the image $I(x, y)$ and a mask filter as illustrated in the following expressions:

$$c_x = [-1 \quad 1] \otimes I(x, y) \quad (4)$$

$$c_y = \begin{bmatrix} -1 \\ 1 \end{bmatrix} \otimes I(x, y) \quad (5)$$

$$c_{xx} = [1 \quad -2 \quad 1] \otimes I(x, y) \quad (6)$$

$$c_{yy} = \begin{bmatrix} 1 \\ -2 \\ 1 \end{bmatrix} \otimes I(x, y) \quad (7)$$

$$c_{xy} = \begin{bmatrix} 1 & -1 \\ -1 & 1 \end{bmatrix} \otimes I(x, y) \quad (8)$$

2.2 External Energy Implementation on FPGA

2.2.1 E_{term}

c_x , c_{xx} , c_y and c_{yy} are the 1D convolutions, each coefficient can be described as illustrated in figure 2 (a, b, c and d) and c_{xy} is the 2D convolution, it can be described as illustrated in figure 2 (e).

2.2.2 $E_{contour}$

It is representing the negative of the square intensity gradient, as shown in figure 3. This energy can be computed using the *Canny* approach, with a

Gaussian mask (3*3) convolved with the image for noise reduction (Canny 1986). We computed horizontal and vertical Sobel masks the same as the Gaussian mask, and the gradient phase can be described by the following equation:

$$\theta = \text{Arctan} \left(\frac{S_y}{S_x} \right) \quad (9)$$

where S_x and S_y are the convolution result with vertical and horizontal Sobel filter respectively.

We considered four values for the phase gradient: 0° , 45° , 90° and 135° , where phase approximation can be described in Table 1. It's simple to compute gradient phase where the multiplication and division is the delay by left and right respectively. Figure 4 can be described by implementation of gradient phase approximation. Non-maximum suppression was used to determine the local maximum pixel value, which is compared to the magnitude of adjacent pixels depending on phase gradient. An example in the following figure (see Fig. 4 a, b and c) can be described by a non-maximum suppression computation.

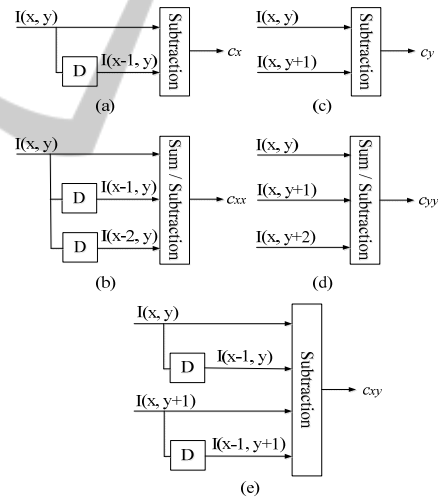


Figure 2: Schema blocks of term energy, (a) Filter by 1D convolution of two coefficients depending on x, (b) Filter by 1D convolution of three coefficients depending on x, (c) Filter by 1D convolution of two coefficients depending on y, (d) Filter by 1D convolution of three coefficients depending on y, (e) Filter by 2D convolution of four coefficients depending on x and y.

A thresholding based on two levels, low and high, called dynamic hysteresis. These two levels vary depending on pixel position. We compute the average of the mask where the center is the pixel position. Dynamic hysteresis thresholding is presented in figure 4.d. We completed architecture of $E_{contour}$ via thresholding step and the preliminary

simulation result represents the efficiency of this new architecture of external energy. A medical image of cancer cells was taken and we applied our active contour implementation. The results of our cancer cell detection are presented in the following section.

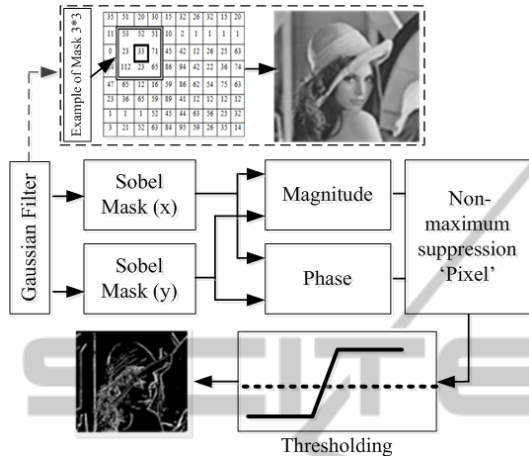


Figure 3: Schema blocks of Canny approach applied on image.

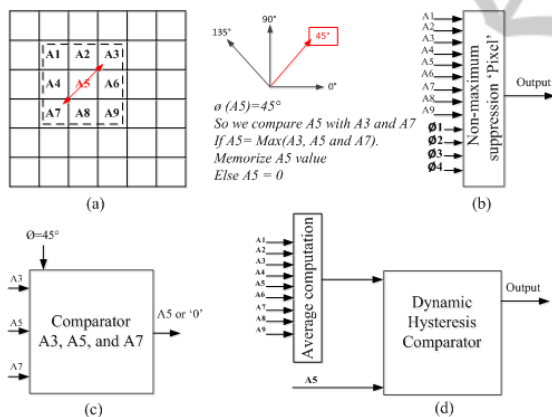


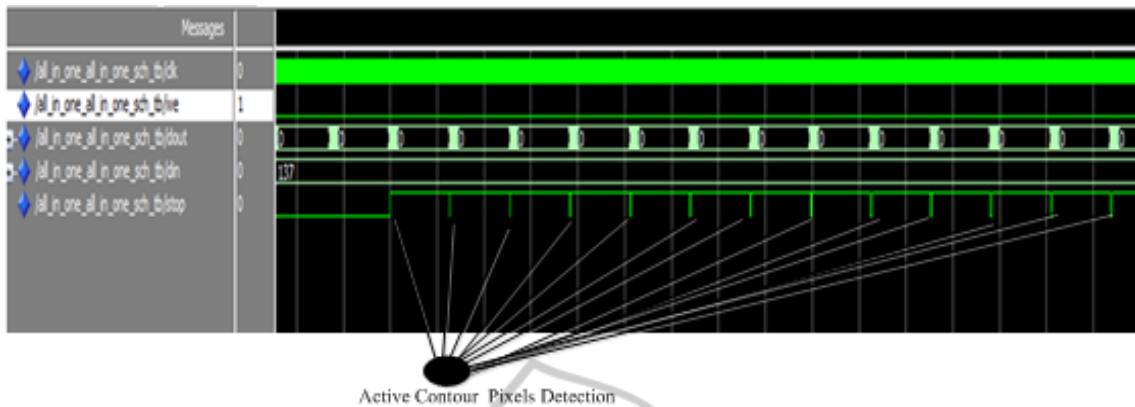
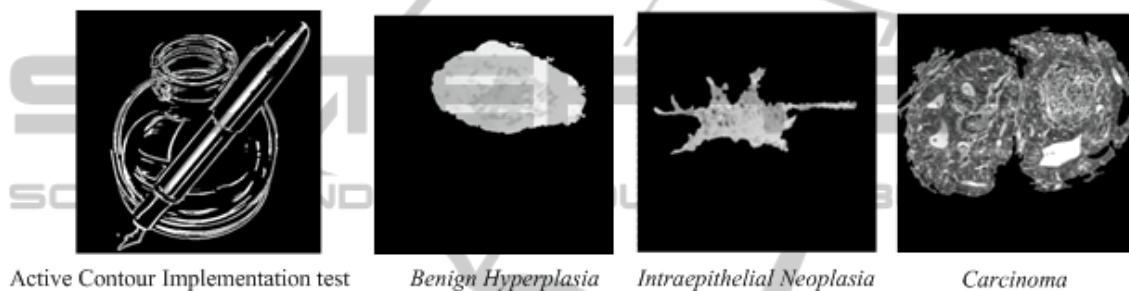
Figure 4: Example of the non-maximum suppression and thresholding computation , (a) example of non-maximum suppression, (b) non-maximum suppression implemented model, (c) block of non-maximum suppression applied of example in (a) and (d) Dynamic hysteresis thresholding model.

Table 1: Proposed approximation of gradient phase.

Gradient phase (θ)	S_y/S_x
$\theta_1 = 0^\circ$ where $0^\circ < \theta < 22.5^\circ$	$0 < S_y < S_x/2$
$\theta_2 = 45^\circ$ where $22.5^\circ < \theta < 67.5^\circ$	$S_x/2 < S_y < 2*S_x$
$\theta_3 = 90^\circ$ where $67.5^\circ < \theta < 112.5^\circ$	$S_y > 2*S_x$
$\theta_4 = 135^\circ$ where $112.5^\circ < \theta < 157.5^\circ$	$-S_x/2 < S_y < -2*S_x$

3 EXPERIMENTAL RESULTS

We provide some results on histopathological images of cell detection (Benign Hyperplasia, Intraepithelial Neoplasia and Carcinoma) to demonstrate the improvements obtained using our architecture. All experiments were done on Xilinx ISE 12.3-FPGA technology using VHDL structural description and Matlab 2012a. Execution time on the order of milliseconds achieved complete active contour. The computation time of processing depends on the type of image, size, and number of objects inside the image. Hence, it is difficult to determine the processing time exactly. However, our goal in this work was to find abnormal cells via active contour in real time using *Xilinx ISE tool* (see Figures 5 and 6). This work is one part of a global project which depends on several constraints such as automatic optical microscopy system, cancer cell detection in real time (Chaddad 2011b, 2013a), and grade classification of cancer cells. Automatic reading of microscopic images includes several consecutive steps in its process. The system must segment an image through detecting and extracting cells from their surrounding medium using morphological image processing. However, the appropriate segmentation technique must be carefully selected to process microscopic images that are high resolution gray scale and multispectral images. Following detection of cells within an image, the system must extract some characteristic parameters in order to distinguish cancerous from normal cells (Chaddad 2011a). The effectiveness of an automatic reading method is generally assessed by its capacity to analyze and interpret a large number of images in a short time. The problem of time computation is still under investigation when there is a need to analyze very large images on different spectral bands. For example, the experimental results in (Sieler 2010) showed that the calculation time for gray level co-occurrence matrix (GLCMs) and Haralick texture features without segmentation step for an image of size 5000*5000 with 16 frequency bands is approximately 350 seconds using a software solution based on a Pentium 4 machine running at 2400 MHz. This effect is directly related to the nature of von Neumann architecture which cannot operate in a parallel fashion. Therefore, in order to reduce the processing time when including the segmentation step, expensive parallel high computing systems based on specific hardware components and large memory storage are designed in order to efficiently compute and perform fast texture analysis

Figure 5: Simulation results from *Xilinx ISE tool*.Figure 6: Simulation results of the active contour implementation using *FPGA* technology.

(Sieler 2010). On the other side, object extraction from shape information in the image is also another important task in biomedical image analysis (Chaddad 2013b). For accurate extraction from very high resolution images, object geometry can be taken into account without the drawback of the prohibitive computation time.

4 CONCLUSIONS

This paper has proposed and implemented an active contour architecture for the detection of abnormal cells. The experimental results showed that the Snake method using the implementation of the Canny approach in external energy provides good performance of cancer cell detection. This architecture applied to images of size 128*128 resulted in highly improved processing times (ms) and can be extended to process larger images of various types. External energy is implemented into a single *FPGA* without the use of any external memory. It also has been proven that by adding new term of Canny approach to the classical Snake method, its performance also increases. The power of this method resides in its ability to detect the

Carcinoma type that was previously difficult to capture it in short time. Therefore, the proposed model of implementation allows accurate and efficient dynamic segmentation of images containing distinct objects in a limited time. This model is useful in automatic segmentation of different histopathological images and thus allowing a faster detection of cancer cells using optical microscopic bio-images. Robust cancer cell detection using optical microscopy is a future continuation of this work. Such an endeavor, which considers many steps, interprets the various supervised methods of classification and detects the cancer cells in a continuous grade in order to treat this malignant disease.

ACKNOWLEDGEMENTS

Authors would like to acknowledge the service *Anapat* of the *CHU* hospital of the Nancy-Brabois and the *Architecture of Embedded Systems and Smart Sensors (ASEC)* team.

REFERENCES

- Castanon, CAB., Fraga, JS., Fernandez, S., Gruber, A., Costa, LF., 2007. Biological shape characterization for automatic image recognition and diagnosis of protozoan parasites of the genus *Eimeria*. *Pat Recog* vol. 40, pp. 1899-1910.
- Wang, X., Li, S., Liu, H., Wood, M., Chen, WR., Zheng, B., 2008. Automated identification of analyzable metaphase chromosomes depicted on microscopic digital images. *J Biomed Inf.*, 41(2):264-71.
- Cataldo, SD., Ficarra, E., Acquaviva, A., Mecii, E. 2010. Achieving the way for automated segmentation of nuclei in cancer tissue images through morphology-based approach: a quantitative evaluation. *Comp Med Imag Graph.*, 34(6):453-61.
- Szilágyi, L., Szilágyi, S.M., Benyó, B., Benyó, Z., 2011. Intensity inhomogeneity compensation and segmentation of MR brain images using hybrid c-means clustering models. *Original Biomedical Signal Processing and Control*, Volume 6, Issue 1, 3-12.
- Chaddad, A., Tanougast, C., Dandache, A., Bouridane, A., 2011. Extracted Haralick's Texture Features and Morphological Parameters from Segmented Multispectral Bio-Images for Classification of Colon Cancer Cells. *WSEAS Transaction on Biology and Biomedicine Journal*, Volume 8, Issue 2, pp. 39-50.
- Chaddad, A., et al., 2012. Evaluation of Different Shape Parameters to Distinguish between Three Abnormally Cancer Types of Cells. *Journal of Computer Vision and Image Processing*, Vol.2, No.4, pp.17-28.
- Kass, M., Witkin, A., Terzopoulos, D., 1988. Snakes: active contour models. *International Journal of Computer Vision*, vol. 1, no. 4, pp. 321-331.
- Caselles, V., et al., 1993. A geometric model for active contours in image processing. *Numerische Mathematik*, vol. 66, no. 1, pp. 1-31.
- Malladi, R., Sethian, JA., Vemuri, BC., 1995. Shape modeling with front propagation: a level set approach. *IEEE Transactions on Pattern Analysis and Machine Intelligence*, vol. 17, no. 2, pp. 158-175.
- He, L., et al., 2008. A comparative study of deformable contour methods on medical image segmentation. *Image and Vision Computing*, vol. 26, no. 2, pp. 141-163.
- Chen, S. Y., Guan, Q., 2011. Parametric shape representation by a deformable NURBS model for cardiac functional measurements. *IEEE Transactions on Biomedical Engineering*, vol. 58, no. 3 PART 1, pp. 480-487.
- Chen, S. Y., Yao, Al., 2012. Recent advances in morphological cell image analysis. *Computational and Mathematical Methods in Medicine*, vol. 2012(2012).
- Canny, J., 1986. A Computational Approach to Edge Detection. *IEEE Transactions on Pattern Analysis and Machine Intelligence*, Vol 8, No. 6, pp. 679-698.
- Chaddad, A., Tanougast, C., Dandache, A., Bouridane, A., 2011. Classification of Cancer Cells Based on Morphological Features from Segmented MultiSpectral Bio-Images. *Recent Advances in Applied & Biomedical Informatics and Computational Engineering in Systems Applications*, August 23-26.
- Chaddad, A., Maamoun, M., Tanougast, C., Dandache, A., 2013. Hardware Implementation of Active Contour Algorithm for Fast Cancer Cells Detection. *IEEE 29th Southern Biomedical Engineering Conference*, May 3-5.
- Sieler, L., Tanougast, C., Bouridane, A., 2010. A scalable and embedded FPGA architecture for efficient computation of Grey Level Co-occurrence Matrices and Haralick textures features. *Microprocess Microsyst.*, 34:14-24.
- Chaddad, A., Tanougast, C., Golato, A., Dandache, A., 2013. Carcinoma cell identification via optical microscopy and shape feature analysis. *Journal of Biomedical Science and Engineering*, 6, pp. 1029-1033.